Numerical Treatment of Two-phase Flow in Porous Media Including Specific Interfacial Area

Procedia Computer Science

Volume 51, 2015, Pages 1249–1258

ICCS 2015 International Conference On Computational Science

Numerical Treatment of Two-Phase Flow in Porous Media Including Specific Interfacial Area

M. F. El-Amin[1]*, R. Meftah[1,2], A. Salama[1], and S Sun[1]

[1] Computational Transport Phenomena Laboratory (CTPL), Division of Physical Sciences and Engineering (PSE), King Abdullah University of Science and Technology (KAUST), Thuwal 23955-6900, Jeddah, Kingdom of Saudi Arabia

[2] University Pierre Marie Curie, Paris, France

mohamed.elamin@kaust.edu.sa

Abstract

In this work, we present a numerical treatment for the model of two-phase flow in porous media including specific interfacial area. For numerical discretization we use the cell-centered finite difference (CCFD) method based on the shifting-matrices method which can reduce the time-consuming operations. A new iterative implicit algorithm has been developed to solve the problem under consideration. All advection and advection-like terms that appear in saturation equation and interfacial area equation are treated using upwind schemes. Selected simulation results such as $p_c - S_w - a_{wn}$ surface, capillary pressure, saturation and specific interfacial area with various values of model parameters have been introduced. The simulation results show a good agreement with those in the literature using either pore network modeling or Darcy scale modeling.

Keywords: Interfacial area, Two-phase flow, Porous media, Capillary pressure, CCFD method, Shifting-matrices method

1 Introduction

The model of flow and transport in porous media, Darcy's law, was originally proposed empirically for one-dimensional isothermal flow of an incompressible fluid in a rigid, homogeneous and isotropic porous medium. The extended Darcy's Law is used for highly complex situations like non-isothermal, multiphase and multicomponent flow and transport, without introducing any additional driving forces. The resisting force, which balances the driving force, is assumed to be linearly proportional to the relative fluid velocity with respect to the solid. This results in a linear relationship between the flow velocity and driving forces. While these assumptions are reasonable for single-phase flow, one may expect many other factors to affect the balance of forces in the case of multiphase flow. Hassanizadeh and Gray [7, 8] developed a unified model

*Corresponding Author

Selection and peer-review under responsibility of the Scientific Programme Committee of ICCS 2015

doi:10.1016/j.procs.2015.05.306

based on rational thermodynamics leading to additional driving forces. The macroscale effects of interfacial forces were included and the momentum balance equations are derived for both phases and interfaces. They found that the driving forces for the flow of a phase were the gradients of Gibbs free energy of the phase plus gravity. In the case of single-phase flow, the gradient of Gibbs free energy reduces to the gradient of pressure. Moreover, capillary pressure is not a hysteretic function of saturation only, but uniquely defined by a capillary pressure-saturation-specific interfacial area surface. In Hassanizadeh and Gray [7], the equations constitute a very complex model that includes many different effects. However, some of these effects are being of second order, whereas several of the involved constitutive relationships have not been investigated so far. In Hassanizadeh and Gray [8], the momentum balance equations were simplified. These studies were followed by a number of other studies (e.g. [9, 10]). Most of these works were done using pore–network modeling and/or experiments and very few attempts were done to simulate the macroscale multiphase flow model including the specific interfacial area such as Ref. [17]. The IMplicit Pressure Explicit Saturation (IMPES) approach solves the pressure equation implicitly and updates the saturation explicitly. In IMPES method, the time step size should be very small, in particular, for highly heterogeneous permeable media. Because the decoupling between the pressure equation and the saturation equation, the IMPES method is conditionally stable. Iterative IMPES splits the equation system into a pressure and a saturation equation that are solved sequentially as IMPES [14, 15, 13].

The objective of this work is to develop an accurate numerical simulator for two-phase flow in porous media including specific interfacial area using appropriate numerical methods. The cell-centered finite difference (CCFD) method together with the shifting-matrices approach are used for spacial discretization, while the upwind scheme is used to treat the advection terms in the differential system.

2 Modeling and Mathematical Formulation

Hassanizadeh and Gray [7] have used a thermodynamic approach using the concept of Gibbs free energy. They concluded that the movement of each phase or interface is governed by its gradient in Gibbs free energy. Now, let us consider the flow of two immiscible and compressible fluids including interfacial area. Assuming that the porosity is constant; the interfacial mass density is constant; the gravity does not have effect on interfacial movement; all material properties are neglected; mass exchange between phases and interfaces has negligible effect on mass balance of phases; and the cross-coupling terms are negligible. Therefore, the governing equations describing the above system can be written as follows [16],

$$\phi\frac{\partial S_\alpha}{\partial t}+\nabla\cdot\mathbf{v}_\alpha=q_\alpha,\quad \alpha=w,n \tag{1}$$

$$\mathbf{v}_\alpha=-\mathbf{K}\frac{k_{r\alpha}}{\mu_\alpha}(\nabla p_\alpha-\rho_\alpha\mathbf{g}),\quad \alpha=w,n \tag{2}$$

$$\frac{\partial a_{wn}}{\partial t}+\nabla\cdot a_{wn}\mathbf{v}_{wn}=E_{wn} \tag{3}$$

$$\mathbf{v}_{wn}=-\mathbf{K}_{wn}\cdot\nabla a_{wn} \tag{4}$$

where ϕ is porosity, S_α, $\mathbf{v}_\alpha$ and q_α denote, respectively, to the saturation, the Darcy's velocity and the source term of the α phase. α stands for the wetting–phase (w) or the nonwetting–phase (n). $\mathbf{K}$ is the intrinsic permeability, μ_α is the dynamic viscosity, $k_{r\alpha}$ denotes the relative

permeability, ρ_α the density and p_α the pressure of the phase α. $a_{wn}[m^{-1}]$ is the specific interfacial area. $\mathbf{v}_{wn}[m \cdot s^{-1}]$ is the interfacial velocity. $\mathbf{K}_{wn}[m^3 \cdot s^{-1}]$ is the interfacial permeability. $E_{wn}[m^{-1} \cdot s^{-1}]$ is the production rate of specific interfacial area. For the production rate of specific interfacial area Joekar-Niasar et al. [11] have defined it as,

$$E_{wn} = -e_{wn} \frac{\partial S_w}{\partial t} \tag{5}$$

To estimate the production rate of specific interfacial area they neglect the advective flux term of Eq.(3). Also the term is calculated as the rate of change of specific interfacial area with time. They defined a linear relationship between E_{wn} and $-\partial S_w/\partial t$. In their work, they also defined e_{wn} as being a linear function of S_w : $e_{wn} = e_1 + e_2 S_w$. The coefficients e_1 and e_2 depend on wetting-phase and non-wetting phase viscosity. On the other hand, in order to close the above system of equations three relations have been added. The first relation is the the sum of wetting-phase and non-wetting phase saturations equals one. The second relation is the difference between non-wetting phase and wetting-phase pressure which is equal to the capillary pressure. The last relation indicates that interfacial specific area is a function of the wetting-phase saturation and the capillary pressure.

$$S_w + S_n = 1 \tag{6}$$

$$p_c = p_n - p_w \tag{7}$$

$$a_{wn} = a_{wn}(S_w, p_c) \tag{8}$$

For the last relation of closure one can use a bi-quadratic relationship depends on S_w and p_c (see Ref. [12]). Instead of the above complicated formula, we will use the following flexible form Ref. [10],

$$a_{wn}(S_w, p_c) = \alpha_1 S_w (1 - S_w)^{\alpha_2} {p_c}^{\alpha_3} \tag{9}$$

where α_1, α_2 and α_3 are constants.

Now, let us define the potential phase α pressure as $\Phi_\alpha = p_\alpha - \rho_\alpha \mathbf{g}$, and the potential capillary pressure as $\Phi_c = p_c - (\rho_n - \rho_w)\,\mathbf{g}$. Also, the total velocity is defined as $\mathbf{v}_t = \mathbf{v}_w + \mathbf{v}_n$, the total mobility $\lambda_t = \lambda_w + \lambda_n$. Adding the saturation equation of wetting phase to the saturation equation of nonwetting phase (1) with the aid of (6), one may obtain,

$$\nabla \cdot \mathbf{v}_t \equiv -\nabla \cdot \lambda_t\,(S_w)\,\mathbf{K}\nabla\Phi_w - \nabla \cdot \lambda_n\,(S_w)\,\mathbf{K}\nabla\Phi_c\,(S_w, a_{nw}) = Q_t \tag{10}$$

where $Q_t = q_w + q_n$. Also, the wetting phase velocity may be defined as,

$$\mathbf{v}_w = -\lambda_w \mathbf{K}\nabla\Phi_w,$$

Therefore, saturation equation of the wetting phase may be written as,

$$\phi \frac{\partial S_w}{\partial t} - \nabla \cdot \lambda_w \mathbf{K}\nabla\Phi_w \equiv \phi \frac{\partial S_w}{\partial t} - \nabla \cdot \mathbf{v}_w = q_w. \tag{11}$$

From (3), (5) and (11), we can write the equation of specific interfacial area as,

$$\phi \frac{\partial a_{nw}}{\partial t} + \phi \nabla \cdot (\mathbf{v}_{wn} a_{nw}) + e_{nw} \nabla \cdot (\mathbf{v}_w) = e_{nw} q_w. \tag{12}$$

The saturation of the wetting phase at the beginning of the flow displacing process is initially defined by,

$$S_w = S_w^0 \qquad \text{at} \quad t = 0. \tag{13}$$

Also, the initial specific interfacial area is zero, i.e.,

$$a_{wn} = a_{wn}^0 \qquad \text{at} \quad t = 0. \tag{14}$$

The general boundary conditions considered in this study are summarized as follow,

$$p_w \,(\text{or } p_n) = p^D \quad \text{on} \quad \Gamma_D, \tag{15}$$

$$\mathbf{v}_t \cdot \mathbf{n} = q^N \quad \text{on} \quad \Gamma_N, \tag{16}$$

$$\mathbf{v}_{wn} \cdot \mathbf{n} = w^N \quad \text{on} \quad \Gamma_N, \tag{17}$$

where Γ_D is the Dirichlet boundary and Γ_N is the Neumann boundary. $\mathbf{n}$ is the outward unit normal vector to Γ_N, p^D is the pressure on Γ_D and q^N the imposed inflow rate on Γ_N, respectively. The saturations on the boundary are subject to,

$$S_w \,(\text{or } S_n) = S^N \quad \text{on} \quad \Gamma_N, \tag{18}$$

and the specific interfacial area on the boundary is subject to,

$$a_{wn} = a_{wn}^N \quad \text{on} \quad \Gamma_N. \tag{19}$$

3 Iterative Implicit Scheme

Define the time step length $\Delta t^n = n^{n+1} - t^n$, the total time interval $[0, T]$ may be divided into N time steps as $0 = t^0 < t^1 < \cdots < t^N = T$. The current time step is represented by the superscript $n+1$. The backward Euler time discretization is used for the equations (10)-(12), to obtain,

$$-\nabla \cdot \lambda_t \left(S_w^{n+1}\right) \mathbf{K} \nabla \Phi_w^{n+1} - \nabla \cdot \lambda_n \left(S_w^{n+1}\right) \mathbf{K} \nabla \Phi_c \left(S_w^{n+1}, a_{nw}^{n+1}\right) = Q_t^{n+1}, \tag{20}$$

$$\phi \frac{S_w^{n+1} - S_w^n}{\Delta t^n} - \nabla \cdot \lambda_w \left(S_w^{n+1}\right) \mathbf{K} \nabla \Phi_w^{n+1} = q_w^{n+1}, \tag{21}$$

and,

$$\phi \frac{a_{nw}^{n+1} - a_{nw}^n}{\Delta t^n} + \phi \nabla \cdot \left(\mathbf{v}_{wn}^{n+1} a_{nw}^{n+1}\right) - e_{nw}^{n+1} \nabla \cdot \lambda_w \left(S_w^{n+1}\right) \mathbf{K} \nabla \Phi_w^{n+1} = e_{nw}^{n+1} q_w^{n+1}. \tag{22}$$

The system (20)–(22) is fully implicit, coupled and highly nonlinear, so it can not be solved directly. Hence, iterative methods are often employed to solve such kind of complicated systems. Now, let us introduce the iterative Implicit Pressure Explicit Saturation-Interfacial Area IMPESA formulation for the equations (20)–(22) that is given as,

$$-\nabla \cdot \lambda_t \left(S_w^{n+1,k}\right) \mathbf{K} \nabla \Phi_w^{n+1,k+1} - \nabla \cdot \lambda_n \left(S_w^{n+1,k}\right) \mathbf{K} \nabla \widetilde{\Phi}_c \left(\widetilde{S}_w^{n+1,k+1}, \widetilde{a}_{nw}^{n+1,k+1}\right) = Q_t^{n+1}, \tag{23}$$

$$\phi \frac{\widetilde{S}_w^{n+1,k+1} - S_w^n}{\Delta t} - \nabla \cdot \lambda_w \left(S_w^{n+1,k}\right) \mathbf{K} \nabla \Phi_w^{n+1,k+1} = q_w^{n+1}, \tag{24}$$

$$\phi\frac{\widetilde{a}_{nw}^{n+1,k+1}-a_{nw}^{n}}{\Delta t^{n}}+\phi\nabla\cdot\left(\mathbf{v}_{wn}^{n+1,k}a_{nw}^{n+1,k}\right)-e_{nw}^{n+1,k}\nabla\cdot\lambda_{w}\left(S_{w}^{n+1,k}\right)\mathbf{K}\nabla\Phi_{w}^{n+1,k+1}=e_{nw}^{n+1,k}q_{w}^{n+1}. \tag{25}$$

The superscripts k and $k+1$ represent the iterative steps within the current time step $n+1$. For each iteration, the variables λ_w, λ_n and λ_t are calculated using the saturation from the previous iteration. However, we may consider the saturation and the specific interfacial area at the current iteration step instead of the previous iteration to obtain the capillary potential Φ_c. We may linearize the capillary potential Φ_c as follows,

$$\begin{aligned}\widetilde{\Phi}_{c}\left(\widetilde{S}_{w}^{n+1,k+1},\widetilde{a}_{nw}^{n+1,k+1}\right)\cong\Phi_{c}\left(S_{w}^{n+1,k},a_{nw}^{n+1,k}\right)+\frac{\partial\Phi_{c}}{\partial S_{w}}\left(S_{w}^{n+1,k},a_{nw}^{n+1,k}\right)\\\left[\widetilde{S}_{w}^{n+1,k+1}-S_{w}^{n+1,k}\right]+\frac{\partial\Phi_{c}}{\partial a_{nw}}\left(S_{w}^{n+1,k},a_{nw}^{n+1,k}\right)\left[\widetilde{a}_{nw}^{n+1,k+1}-a_{nw}^{n+1,k}\right]\end{aligned} \tag{26}$$

The changes of saturation and interfacial area in a time step are often very small, and hence the linear approximation is reasonable. Moreover, the relaxation approach is often applied to control the convergence of nonlinear iterative solvers. In this algorithm we use the following two relaxation relationships for saturation and interfacial area as,

$$S_{w}^{n+1,k+1}=S_{w}^{n+1,k}+\theta_{s}\left(\widetilde{S}_{w}^{n+1,k+1}-S_{w}^{n+1,k}\right), \tag{27}$$

and,

$$a_{nw}^{n+1,k+1}=a_{nw}^{n+1,k}+\theta_{a}\left(\widetilde{a}_{nw}^{n+1,k+1}-a_{nw}^{n+1,k}\right), \tag{28}$$

where $\theta_s, \theta_a \in (0,1]$ are relaxation factors.

4 Spatial Discretization

Now, let us apply the CCFD scheme to the system of equations (23)–(28) to obtain the iterative discretization. The discretization form of the pressure equation may be given as,

$$\mathbf{A}_{wt}\left(S_{w}^{n+1,k}\right)\mathbf{\Phi}_{w}^{n+1,k+1}+\mathbf{A}_{c}\left(S_{w}^{n+1,k}\right)\mathbf{P}_{c}\left(\widetilde{S}_{w}^{n+1,k+1},\widetilde{a}_{nw}^{n+1,k+1}\right)=\mathbf{Q}_{ct}^{n+1}. \tag{29}$$

It is noted from above algebraic equations that the matrices $\mathbf{A}_w$ and $\mathbf{A}_c$ depend on the vector $S_w^{n+1,k}$ at the previous iteration step, while the vector $\mathbf{P}_c$ depends on both vectors $S_w^{n+1,k+1}$ and $a_{nw}^{n+1,k+1}$ at the current iteration step, which may be written as, in a matrix-vector form as follows,

$$\begin{aligned}\widetilde{\mathbf{P}}_{c}\left(\widetilde{S}_{w}^{n+1,k+1},\widetilde{a}_{nw}^{n+1,k+1}\right)\cong\mathbf{\Phi}_{c}\left(S_{w}^{n+1,k},a_{nw}^{n+1,k}\right)+\mathbf{P}_{s}\left(S_{w}^{n+1,k},a_{nw}^{n+1,k}\right)\\\left[\widetilde{\mathbf{S}}_{w}^{n+1,k+1}-\mathbf{S}_{w}^{n+1,k}\right]+\mathbf{P}_{a}\left(S_{w}^{n+1,k},a_{nw}^{n+1,k}\right)\left[\widetilde{\mathbf{a}}_{nw}^{n+1,k+1}-\mathbf{a}_{nw}^{n+1,k}\right]\end{aligned} \tag{30}$$

where the matrices $\mathbf{P}_s$ and $\mathbf{P}_a$ are diagonal resulted from the discretization of $\frac{\partial\Phi_c}{\partial S_w}$ and $\frac{\partial\Phi_c}{\partial a_{nw}}$, respectively. In fact, the derivatives of $\mathbf{\Phi}_c$ are viewed as functions of $\mathbf{\Phi}_c$ when the saturation and the interfacial area at each spatial point vary with time. At the same time, the saturation and the interfacial area are smoothly changing along with time at each spatial point even they are discontinuously distributed in space.

Also, the CCFD discretization of the saturation equation (24) may lead to,

$$\mathbf{M}\frac{\widetilde{\mathbf{S}}_{w}^{n+1,k+1}-\mathbf{S}_{w}^{n}}{\Delta t^{n}}+\mathbf{A}_{w}\left(S_{w}^{n+1,k}\right)\mathbf{\Phi}_{w}^{n+1,k+1}=Q_{w}^{n+1}, \tag{31}$$

where $\mathbf{M}$ is a diagonal matrix replaces the porosity that appears in the saturation equation and also it is a function of cell area. It is worth mentioning that the above equation of saturation is coupled with the pressure equation to be solved implicitly together, however it is not used to update the saturation.

Similarly, the CCFD discretization of the interfacial area equation (25) can be given as,

$$\begin{gathered}\mathbf{M}\frac{\widetilde{\mathbf{a}}_{nw}^{n+1,k+1}-\mathbf{a}_{nw}^{n}}{\Delta t^{n}}+\mathbf{M}\left[\mathbf{A}_{nw,a}\left(a_{nw}^{n+1,k}\right)\mathbf{a}_{nw}^{n+1,k}+\mathbf{A}_{nw,s}\left(a_{nw}^{n+1,k}\right)\mathbf{S}_{w}^{n+1,k}\right]+\\ \mathbf{E}\left(S_{w}^{n+1,k}\right)\mathbf{A}_{w}\left(S_{w}^{n+1,k}\right)\mathbf{\Phi}_{w}^{n+1,k+1}=\mathbf{E}\left(S_{w}^{n+1,k}\right)\mathbf{Q}_{w}^{n+1},\end{gathered} \tag{32}$$

where $\mathbf{E}\left(S_{w}^{n+1,k}\right)$ is a diagonal matrix.

The above equation of saturation is coupled with the pressure equation to be solved implicitly together, however it is not used to update the saturation. Substituting from (30)-(32) into (29), the coupled pressure equation becomes,

$$\mathbf{A}_{t}\left(S_{w}^{n+1,k},a_{nw}^{n+1,k}\right)\mathbf{\Phi}_{w}^{n+1,k+1}=\mathbf{Q}_{t}\left(S_{w}^{n+1,k},a_{nw}^{n+1,k}\right). \tag{33}$$

where

$$\begin{gathered}\mathbf{A}_{t}\left(S_{w}^{n+1,k},a_{nw}^{n+1,k}\right)=\mathbf{A}_{wt}-\Delta t^{n}\mathbf{A}_{c}\left(S_{w}^{n+1,k}\right)\left[\mathbf{P}_{s}\left(S_{w}^{n+1,k},a_{nw}^{n+1,k}\right)\mathbf{M}^{-1}+\right.\\ \left.\mathbf{P}_{a}\left(S_{w}^{n+1,k},a_{nw}^{n+1,k}\right)\mathbf{M}^{-1}\mathbf{E}\right]\mathbf{A}_{w}\left(S_{w}^{n+1,k}\right)\end{gathered} \tag{34}$$

and

$$\begin{gathered}\mathbf{Q}_{t}\left(S_{w}^{n+1,k},a_{nw}^{n+1,k}\right)=\mathbf{Q}_{ct}^{n+1}-\mathbf{A}_{c}\left(S_{w}^{n+1,k}\right)\left\{\mathbf{\Phi}_{c}\left(S_{w}^{n+1,k}\right)+\right.\\ \mathbf{P}_{s}\left(S_{w}^{n+1,k}\right)\left(\mathbf{S}_{w}^{n}-\mathbf{S}_{w}^{n+1,k}\right)+\mathbf{P}_{a}\left(S_{w}^{n+1,k}\right)\left(\mathbf{a}_{nw}^{n}-\mathbf{a}_{aw}^{n+1,k}\right)\\ -\Delta t^{n}\mathbf{P}_{a}\left(S_{w}^{n+1,k}\right)\left[\mathbf{A}_{nw,a}\left(a_{nw}^{n+1,k}\right)\mathbf{a}_{nw}^{n+1,k}+\mathbf{A}_{nw,s}\left(a_{nw}^{n+1,k}\right)\mathbf{S}_{w}^{n+1,k}\right]+\\ \left.\Delta t^{n}\left[\mathbf{P}_{s}\left(S_{w}^{n+1,k},a_{nw}^{n+1,k}\right)\mathbf{M}^{-1}+\mathbf{P}_{a}\left(S_{w}^{n+1,k},a_{nw}^{n+1,k}\right)\mathbf{M}^{-1}\mathbf{E}\right]\mathbf{Q}_{w}^{n+1}\right\}.\end{gathered} \tag{35}$$

After updating the velocity $\mathbf{u}_{w}^{n+1,k+1}$, we can update the saturation, we consider the following explicit scheme,

$$\phi\frac{S_{w}^{n+1,k+1}-S_{w}^{n}}{\Delta t^{n}}+\nabla\cdot\mathbf{u}_{w}^{n+1,k+1}=q_{w}^{n+1}. \tag{36}$$

Now, we can update all variables that are functions in S_w. Then, after updating $\mathbf{w}_{nw}^{n+1,k+1}$, the interfacial area can be updated by the following explicit scheme,

$$\phi\frac{a_{nw}^{n+1,k+1}-a_{nw}^{n}}{\Delta t^{n}}+\phi\nabla\cdot\left(\mathbf{w}_{nw}^{n+1,k+1}a_{nw}^{n+1,k}\right)+e_{nw}^{n+1,k+1}\nabla\cdot\mathbf{u}_{w}^{n+1,k+1}=e_{nw}^{n+1,k+1}q_{w}^{n+1}. \tag{37}$$

The upwind CCFD discretization of the above two equations (36) and (37) are,

$$\mathbf{M}\frac{\widetilde{\mathbf{S}}_{w}^{n+1,k+1}-\mathbf{S}_{w}^{n}}{\Delta t^{n}}+\mathbf{A}_{\mathbf{u}}\left(S_{w}^{n+1,k},a_{nw}^{n+1,k}\right)=\mathbf{Q}_{s}^{n+1}, \tag{38}$$

and,

$$\mathbf{M}\frac{\widetilde{\mathbf{a}}_{nw}^{n+1,k+1}-\mathbf{a}_{nw}^{n}}{\Delta t^{n}}+\mathbf{M}\mathbf{A}_{\mathbf{w}}\left(S_{w}^{n+1,k},a_{nw}^{n+1,k}\right)\mathbf{a}_{nw}^{n+1,k}+\mathbf{E}\mathbf{A}_{\mathbf{u}}\left(S_{w}^{n+1,k},a_{nw}^{n+1,k}\right)=\mathbf{E}\mathbf{Q}_{a}^{n+1}, \tag{39}$$

respectively.

The Shifting–Matrices method [19] is used in the implementation of the above discretized system.

5 Numerical Experiments

This section analyzes some results of saturation, capillary pressure and specific interfacial area. For example, we choose fluid parameters (densities, viscosities, and diffusion constants) of water and air; for the matrix parameters, we take typical soil parameters, here $k = 10^{-10}\mathbf{m^2}$ and $\phi = 0.3$. We take a rough estimate of $k_{nw} = 10^{-5}\ \mathbf{m^3 s^{-1}}$. We set the interfacial permeability K_{wn} to $10^{-5}\ m^3/s$. The ratio between non-wetting phase and wetting-phase viscosity is $\mu_n/\mu_w = 0.1$. The coefficients for the production rate of specific interfacial area we use the values from Ref. [10]. The initial condition for the specific interfacial a_{wn} is taken as 5790 $[1/m]$ and at the boundary conditions are given as: 1000 $[1/m]$ on the west boundary; 5790 $[1/m]$ on the east boundary; and 0 $[1/m]$ on the north and south boundary. Also, the boundary conditions of the interface velocity v_{wn}, is considered 0.001 $[m/year]$ on the west boundary and 0 $[m/year]$ on the east, north and south boundaries. The parameters in the capillary pressure formula are set to $\alpha_1 = 250\ 000$, $\alpha_2 = 1.18$ and $\alpha_3 = -0.8$. Figure 1 represents relation between specific interfacial area, saturation and capillary pressure. It is interesting to note that this 3D surface is comparable to previous experimental and computational studies, [1, 10, 18]. Figure 2**(a)** shows the variation of capillary pressure with saturation. From this figure we may conclude that the capillary pressure increases with decreasing wetting-phase saturation. The variations of the specific interfacial area with wetting-phase saturation are plotted in Fig. 2**(b)**. According to this figure, one can observe that the specific interfacial area decreases with increasing the wetting-phase saturation.

In another example, we choose counter-current imbibition model [3, 4, 5, 6, 2]. In the case of considering the specific–interfacial–area, the capillary pressure formula $p_c(S_w, a_{wn})$ is very sensitive to its parameters. The values of these parameters may be modified based on the type of porous media and other physical and computational aspects. So, here we investigate the sensitivity of the capillary pressure parameters, namely, α_1, α_2 and α_3. In Fig. 3a, the specific interfacial area is plotted against the capillary pressure with different values of α_1, at $\alpha_2 = 1.18$ and $\alpha_3 = -0.8$. This figure shows that the specific interfacial area could has same values for different capillary pressure ranges based on the values of the parameter α_1. Fig. 3b shows the specific interfacial area profiles against the capillary pressure with various values of the parameter α_2, at $\alpha_1 = 2.5 \times 10^7$ and $\alpha_3 = -0.8$. It is interesting to note from Fig. 3b that the behavior of the interfacial area profiles with small values of α_2 is totally different from those with bigger values of α_2. The specific interfacial area decreases as the parameter α_2 decreases and opposite is true for the capillary pressure. The specific interfacial area is plotted in Fig. 3c against the capillary pressure with different values of α_3, at $\alpha_1 = 2.5 \times 10^7$ and $\alpha_2 = 1.18$. It can be seen from this figure that as the parameter α_3 increases the interfacial area slightly increases with bigger values of the capillary pressure. Also, Fig. Fig. 3c illustrates the capillary pressure variation against the water saturation at different values of α_1, at $\alpha_2 = 1.18$ and $\alpha_3 = -0.8$. It is clear from this figure that as the parameter α_1 increases the capillary pressure increases. Moreover, it is interesting to note from the same figure that the capillary pressure has reasonable physical values of $\alpha_1 \geq \mathbf{o}(10^5)$. The profiles of the capillary pressure are plotted in Fig. 3d against the water saturation with different values of the parameter $\alpha_2 = 0.01 : 2.5$, at $\alpha_1 = 2.5 \times 10^7$ and $\alpha_3 = -0.8$. It is clear here that when $\alpha_2 > 1$, the behavior of the $P_c - S$ curve deviates from the standard behavior. Fig. 3e shows the capillary pressure against the water saturation with different values of the α_3, with $\alpha_1 = 2.5 \times 10^7$ and $\alpha_2 = 1.18$. From Fig. 3f, it can be noted that the behavior of the $P_c - S$ curve deviates from the standard behavior at $\alpha_3 > -0.8$.

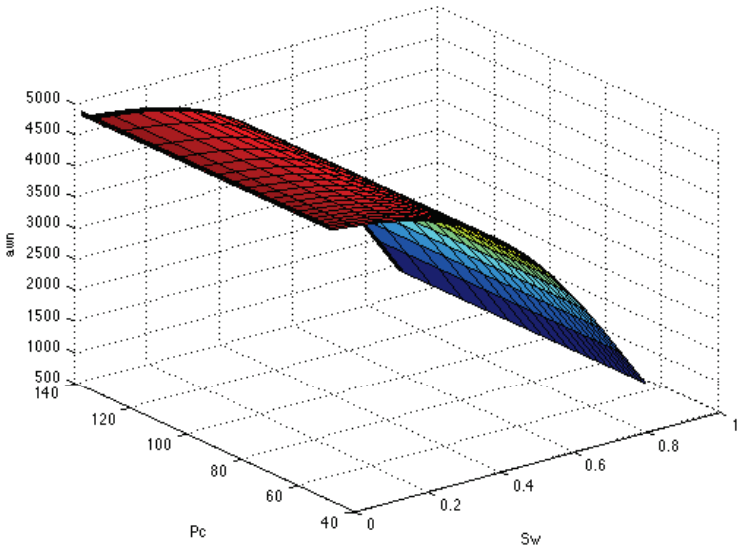

Figure 1: Distribution of $S_w - p_c - a_{wn}$ surface

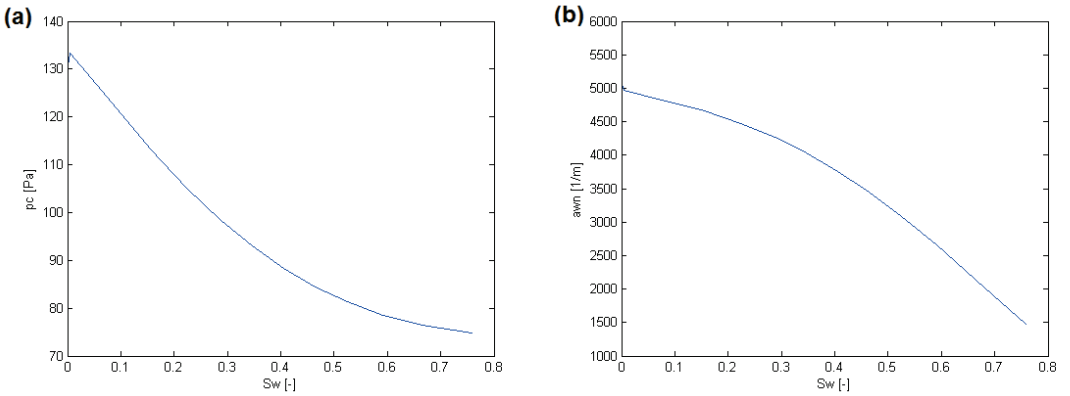

Figure 2: Variation of **(a)** capillary pressure with saturation, and **(b)** Variation of specific interfacial area with saturation

References

[1] J. T. Cheng, L. J. Pyrak-Nolte, D. D. Nolte, and N. J. Giordano. Linking pressure and saturation through interfacial areas in porous media. *Geophysical Research Letters*, 31(8), 2004.

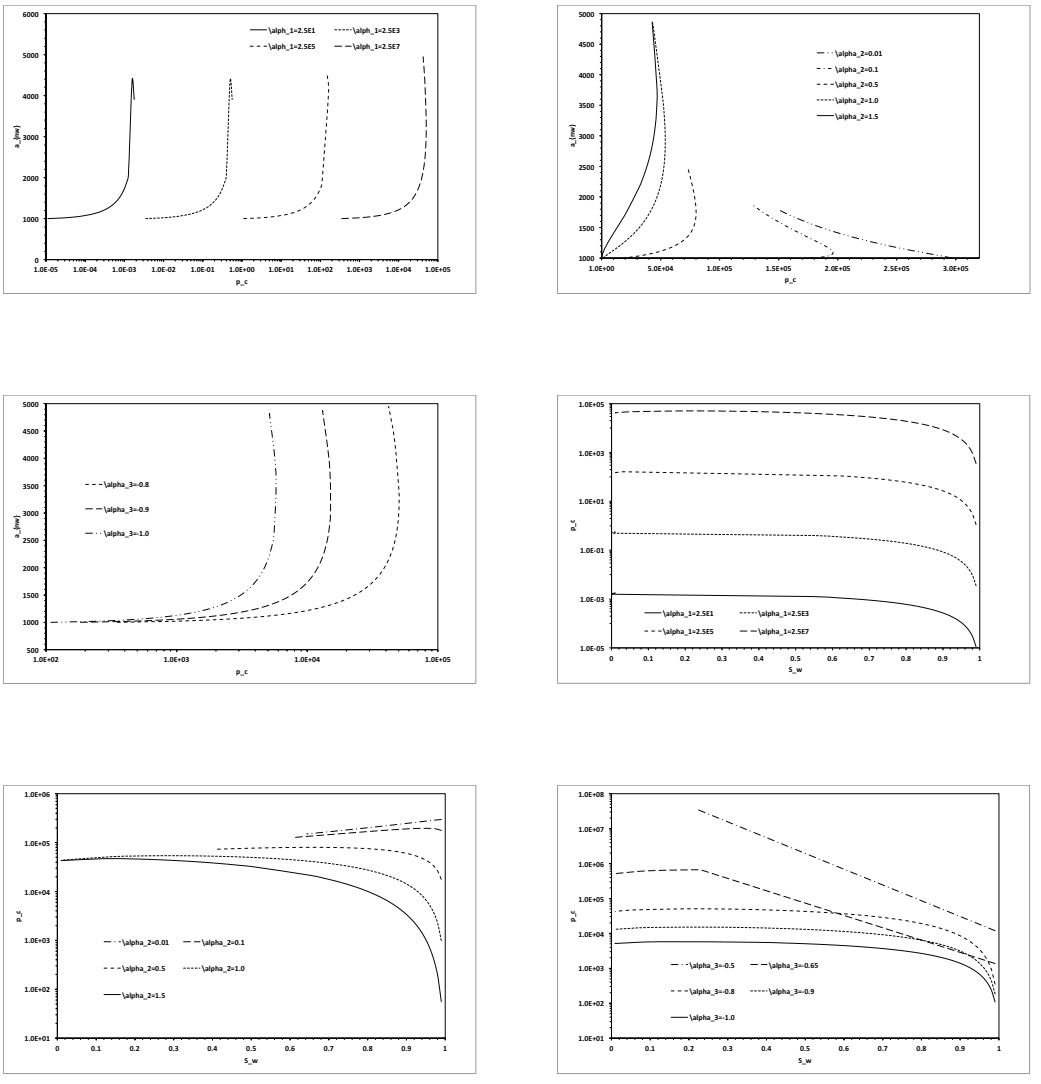

Figure 3: Variation of capillary pressure, saturation and specific interfacial area with various values of α_1, α_2 and α_3

[2] M. F. El-Amin, A. Salama, and S. Sun. Effects of gravity and inlet location on a two-phase countercurrent imbibition in porous media. *International Journal of Chemical Engineering*, 2012, 2012.

[3] M. F. El-Amin, A. Salama, and S. Sun. A generalized power-law scaling law for a two-phase imbibition in a porous medium. *Journal of Petroleum Science and Engineering*, 111(0):159 – 169, 2013.

[4] M. F. El-Amin, A. Salama, and S. Sun. Numerical and dimensional investigation of two-phase countercurrent imbibition in porous media. *Journal of Computational and Applied Mathematics*, 242(0):285 – 296, 2013.

[5] M. F. El-Amin, A. Salama, and S. Sun. Numerical and dimensional analysis of nanoparticles transport with two-phase flow in porous media. *Journal of Petroleum Science and Engineering*, 128(0):53 – 64, 2015.

[6] M. F. El-Amin and S. Sun. Effects of gravity and inlet/outlet location on a two-phase cocurrent imbibition in porous media. *Journal of Applied Mathematics*, 2011, 2011.

[7] S. M. Hassanizadeh and W. G. Gray. Mechanics and thermodynamics of multiphase flow in porous media including interphase boundaries. *Advances in Water Resources*, 13:169–186, 1990.

[8] S. M. Hassanizadeh and W. G. Gray. Thermodynamic basis of capillary pressure in porous media. *Water Resources Research*, 29(10):3389–3405, 1993.

[9] R. J. Held and M. A. Celia. Modeling support of functional relationships between capillary pressure, saturation, interfacial area and common lines. *Advances in Water Resources*, 24(3–4):325–343, 2001/3// 2001.

[10] V. Joekar-Niasar and S. M. Hassanizadeh. Uniqueness of specific interfacial area–capillary pressure–saturation relationship under non-equilibrium conditions in two-phase porous media flow. *Transport in Porous Media*, 94(2):465–486, 2012.

[11] V. Joekar Niasar, S. M. Hassanizadeh, and H. K. Dahle. Non-equilibrium effects in capillarity and interfacial area in two-phase flow: dynamic pore-network modelling. *Journal of Fluid Mechanics*, 655:38–71, 7 2010.

[12] V. Joekar-Niasar, S. M. Hassanizadeh, and A. Leijnse. Insights into the relationships among capillary pressure, saturation, interfacial area and relative permeability using pore-network modeling. *Transport in Porous Media*, 74(2):201–219, 2008.

[13] J. Kou and S. Sun. On iterative impes formulation for two phase flow with capillarity in heterogeneous porous media. *International Journal of Numerical Analysis and Modeling. Series B*, 1(1):20–40, 2010.

[14] S. Lacroix, Y. Vassilevski, J. Wheeler, and M. F. Wheeler. Iterative solution methods for modeling multiphase flow in porous media fully implicitly. *SIAM Journal on Scientific Computing*, 25(3):905–926, 2003.

[15] B. Lu and M. F. Wheeler. Iterative coupling reservoir simulation on high performance computers. *Petroleum Science*, 6(1):43–50, 2009.

[16] J. Niessner and S. M. Hassanizadeh. A model for two-phase flow in porous media including fluid-fluid interfacial area. *Water Resources Research*, 44(8), 2008.

[17] I. S. Pop, C. J. van Duijn, J. Niessner, and S. M. Hassanizadeh. Horizontal redistribution of fluids in a porous medium: The role of interfacial area in modeling hysteresis. *Advances in Water Resources*, 32(3):383 – 390, 2009.

[18] M. L. Porter, D. Wildenschild, G. Grant, and J. I. Gerhard. Measurement and prediction of the relationship between capillary pressure, saturation, and interfacial area in a napl-water-glass bead system. *Water Resources Research*, 46(8), 2010.

[19] S. Sun, A. Salama, and M. F. El Amin. Matrix-oriented implementation for the numerical solution of the partial differential equations governing flows and transport in porous media. *Computers and Fluids*, 68(0):38 – 46, 2012.